Residual-based *a posteriori* error estimation for stochastic magnetostatic problems

D.H. Mac[a], Z. Tang[b], S. Clénet[a], E. Creusé[c]

[a] *L2EP/Arts et Métiers ParisTech centre Lille, 8 bd Louis 14, 59000 Lille, France.*
[b] *L2EP/Université Lille Nord de France, Cité Scientifique, 59655 Villeneuve d'Ascq Cedex, France.*
[c] *Laboratoire Paul Painlevé/Université Lille Nord de France* & INRIA Lille Nord Europe (EPI MEPHYSTO), Cité Scientifique, 59655 Villeneuve d'Ascq Cedex, France.

Abstract

In this paper, we propose an *a posteriori* error estimator for the numerical approximation of a stochastic magnetostatic problem, whose solution depends on the spatial variable but also on a stochastic one. The spatial discretization is performed with finite elements and the stochastic one with a polynomial chaos expansion. As a consequence, the numerical error results from these two levels of discretization. In this paper, we propose an error estimator that takes into account these two sources of error, and which is evaluated from the residuals.

Keywords:
Residual-based a posteriori error estimate, stochastic partial differential equation, finite element method, polynomial chaos expansion, stochastic spectral finite element method.

1. Introduction

Nowadays, numerical simulation is often used to predict the behavior of physical systems. The mathematical equations describing the physical phenomena under consideration are solved by using a numerical method such as the Finite Element Method (FEM). The input data of the numerical model are usually defined as the dimensions of the device, the behavior law of the materials and the sources. The information on these input data is available with some uncertainties due to several factors such as the imperfections of the manufacturing processes, the ageing of the material or the influence of

the exterior environment. As long as the error due to the approximation is large enough, the impact of the uncertainties on the output results can be considered as negligible, leading to a deterministic problem. Nevertheless, this assumption is no more always valid because of the high reduction of the numerical error due to the progress in the numerical analysis domain and to the increasing capabilities of the computers. Therefore, for a better description of the realistic physical system, the uncertainties of the input data have to be taken into account.

A probabilistic approach [2, 6, 7, 18, 20] is one possibility for accounting for uncertainties on the inputs and to characterize their influence on the outputs. In this approach, the uncertain quantities are modeled by random variables (or random fields). There are two steps to be followed. The first step consists in modeling the input data by random variables (or random fields) with known probability density functions. In the second step, these uncertainties are propagated through the numerical model to quantify their effects on the outputs. Many methods are proposed in the literature to deal with this second step [2, 6, 7, 12, 13, 18, 19, 20].

In a stochastic problem, the solution of the mathematical equations depends on the spatial dimension as well as the stochastic one. In [12, 13, 19, 20] a spatial discretization using finite elements along with a stochastic discretization using polynomial chaos [29] is used to approximate the stochastic solution. When the stochastic solution is approximated explicitly as a function of the spatial dimension and the stochastic dimension, the statistics of the output response can be characterized easily in the postprocessing step.

The reliability of the characteristics of the output data depends obviously on the accuracy of the approximated solution. In this paper, we are interested in an *a posteriori* error estimation. This kind of error estimation (compared to an *a priori* error estimation) is evaluated from the numerical solution and does not depend on the exact solution, in particular on its regularity.

The analysis of the error due to the spatial discretization has already been performed in the pure deterministic case. In [1], an error estimation based on the gradient recovery method is proposed. The principle of this method is that one can build an approximation of the gradient of the exact solution from the numerical solution. The error estimation is obtained by evaluating the distance between this approximated gradient and the gradient of the numerical solution itself. Some techniques to build this approximated gradient were proposed in [4, 30, 31].

In [24], the error estimation is based on the hypercycle principle (equi-

librated error estimation) and evaluated from two admissible fields coming from the numerical solutions of two complementary formulations.

In [3, 5, 8, 9], the error estimation is derived by solving the error equation with the right hand-side being a residual evaluated from the numerical solution (implicit residual method). The equation on the error can be global [8, 9] or local [3, 5] and must be solved in a richer basis (finer mesh or higher order of the shape functions).

In [10], the distance between the approximated value of a global quantity (obtained from the numerical solution) and its exact value (obtained from the exact solution) is estimated by introducing a dual problem. Both approximated and exact solutions of the dual problem are required. Actually, the exact solution of the dual problem is replaced by another approximated solution obtained using a richer basis.

In [27], an explicit residual method is proposed. This method is different from the implicit residual method in that the error estimation is evaluated directly from the residual. Therefore, the computational cost of the error estimation is much smaller. However, the true magnitude of the real approximation error is not available due to some non explicit constants appearing in the development of this kind of error estimator.

Inspired by the above method for deterministic problem, some methods have been proposed to deal with the stochastic case. In [17], due to the fact that the approximated stochastic solutions obtained from two complementary formulations are also admissible, an equilibrated error estimator has been proposed. This error estimator provides a global estimation of the error but does not allow to distinguish the spatial contribution from the stochastic one.

In [23], an error estimation based on the solution of a dual problem is proposed. The interesting point in this paper is that for some initial nonlinear problems, the dual problem becomes linear. Therefore, the solution of the dual problem needs much less time than the initial one. The error estimation in [23] is also global and it is applicable only for the numerical solution obtained by the Spectral Stochastic Finite Element Method (SSFEM)[12, 19, 20].

In [28] an error estimator based on the implicit residual method is proposed. A richer basis in the stochastic dimension is applied using polynomials of higher order than the ones used for the solution. An error estimator evaluated from the stochastic residual and the mean value of the stiffness matrix has also been proposed recently in [22]. These papers [22, 28] focus on the stochastic error and the spatial error is assumed to be negligible.

In this paper, the explicit residual method in the deterministic case [27] is extended to the stochastic case. Our purpose is to propose an error estimation that splits the stochastic and the spatial errors. The paper is organized as follows. In section 2, the functional spaces are defined. In section 3, we define the deterministic magnetostatic problem, and the problem is extended to the stochastic case. Some methods to approximate the stochastic solution are briefly recalled. Section 4 is devoted to the derivation of the error estimator. We will show that the stochastic error can be bounded by a term including the stochastic residual. Then, an estimation of the global error is proposed where the stochastic and the spatial error are separated. In section 5, a numerical application illustrates the obtained theoretical results.

2. Functional spaces definition

We are interested in a magnetostatic problem defined in a polyhedral domain $\mathrm{D} \subset \mathbb{R}^3$ with uncertainties on the material behavior law. A probabilistic approach [20] is used to take into account the effect of these uncertainties on the output data. We introduce then the probability space $(\Xi, F, \mathbb{P})$ where Ξ is the set of elementary events, F is a σ-algebra on Ξ and $\mathbb{P}$ is a probability measure. For a given vector of M independent random variables $\boldsymbol{\xi} : \Xi \to \Theta^M \subset \mathbb{R}^M$, where M is a positive integer, we introduce also the space $V_{\boldsymbol{\xi}}$ of real functions defined in Θ^M :

$$V_{\boldsymbol{\xi}} = \{u|\ \mathrm{E}[u^2] = \int_{\Theta^M} |u(x)|^2 f_{\boldsymbol{\xi}}(x)\ dx < \infty\}, \tag{1}$$

where $\mathrm{E}[u]$ is the expectation of the random variable u and $f_{\boldsymbol{\xi}}$ the probability density function of $\boldsymbol{\xi}$, assumed to be defined. The dot product on $V_{\boldsymbol{\xi}}$ is defined by:

$$\langle u, v \rangle_{V_{\boldsymbol{\xi}}} = \int_{\Theta^M} u(x)v(x)f_{\boldsymbol{\xi}}(x)\ dx. \tag{2}$$

In [15, 29], it is shown that a set of polynomial chaos $\{\Psi_{\boldsymbol{\alpha}}|\ \boldsymbol{\alpha} \in \mathbb{N}^M\}$ defines a basis of the Hilbert space $V_{\boldsymbol{\xi}}$, meaning that all $u \in V_{\boldsymbol{\xi}}$ admits a unique decomposition:

$$u(\boldsymbol{\xi}) = \sum_{\boldsymbol{\alpha} \in \mathbb{N}^M} u_{\boldsymbol{\alpha}} \Psi_{\boldsymbol{\alpha}}(\boldsymbol{\xi}) \tag{3}$$

with $u_{\boldsymbol{\alpha}} = \mathrm{E}[u(\boldsymbol{\xi})\Psi_{\boldsymbol{\alpha}}(\boldsymbol{\xi})]$ and $\mathbb{N}$ the set of natural numbers. For $P \in \mathbb{N}^*$ we define a finite dimension sub-space $V_{\boldsymbol{\xi}}^P \subset V_{\boldsymbol{\xi}}$ by:

$$V_{\boldsymbol{\xi}}^P = \mathrm{span}\left\{ \Psi_{\boldsymbol{\alpha}} |\ \boldsymbol{\alpha} \in K_P = (\alpha_1, \alpha_2, ..., \alpha_M) \in \mathbb{N}^M \mid \sum_{k=1}^{M} \alpha_k \leqslant P \right\}. \tag{4}$$

Here, P denotes the order of the polynomial chaos. We denote $L^2(D)$ the space of real scalar square integrable functions defined on D. We introduce the functional spaces:

$$\begin{aligned} V_x &= \left\{ u \in L^2(D)\ ;\ \int_D |\mathbf{grad}\ u(x)|^2\, dx < \infty \right\}, \\ V_x^0 &= \left\{ u \in V_x\ ;\ \int_D u(x)\, dx = 0 \right\}. \end{aligned} \tag{5}$$

We denote by $\mathcal{T}_h$ a spatial tetrahedral mesh of the domain D which is regular in the Ciarlet sense (that is to say that for each of the tetrahedra, the ratio between its diameter and the diameter of its largest inscribed ball is uniformly bounded). Here, the index h arising in $\mathcal{T}_h$ characterizes the accuracy of the mesh, defined as the maximum value of all the diameters of the tetrahedra in the mesh. The mesh is composed of n_0 nodes, n_1 edges, n_2 facets and n_3 tetrahedral elements. We define the following discrete functional spaces on $\mathcal{T}_h$ [14]:

$$V_x^h = \mathrm{span}\{w_{0i}\ , i = 1 : n_0\}, \tag{6}$$

$$V_x^{hi_0} = \mathrm{span}\{w_{0i}\ , i = 1 : n_0, i \neq i_0\}, \tag{7}$$

$$V_x^{h0} = \left\{ u \in V_x^h |\ \int_D u(x)\ dx = 0 \right\}, \tag{8}$$

where w_{0i} is the usual first order nodal shape function associated with the node i, and i_0 is a given arbitrary node of $\mathcal{T}_h$. The tensorial functional space is defined by the following way:

$$V_x \otimes V_{\boldsymbol{\xi}} = \{u |\ \forall x \in D,\ u(x, .) \in V_{\boldsymbol{\xi}} \text{ and } \forall \boldsymbol{\xi} \in \Theta^M,\ u(., \boldsymbol{\xi}) \in V_x\}. \tag{9}$$

3. Magnetostatic problem

In this section, we first present the deterministic magnetostatic problem and its numerical approximation by the Finite Element Method (FEM). It

will be the starting point to derive our error estimator for the stochastic magnetostatic problem. We then introduce the stochastic magnetostatic problem. Some numerical methods to deal with this problem are briefly discussed.

3.1. Deterministic magnetostatic problem

The deterministic magnetostatic problem is defined on a polyhedral domain D (cf. Fig. 1) where the permeability at point x is denoted by $\mu(x)$.

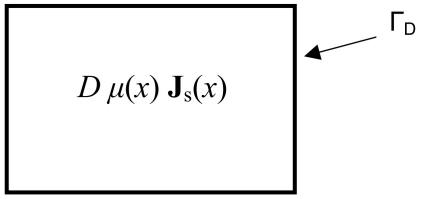

Figure 1: Magnetostatic problem defined on the domain D.

The boundary of D is denoted by Γ_D. A stranded inductor is fed by a divergence free current density $\mathbf{J}_s$. A source field $\mathbf{H}_s$ is introduced such that curl $\mathbf{H}_s(x) = \mathbf{J}_s(x)\ \forall x \in D$. In this paper, we suppose that this source field can be written in the following form:

$$\mathbf{H}_s(x) = \sum_{i=1}^{n_1} \gamma_i\ \mathbf{w}_{1i}(x), \tag{10}$$

where $\mathbf{w}_{1i}$ is the usual first order Nédélec shape function associated with the edge i of the mesh $\mathcal{T}_h$ [14] and $\gamma_i \in \mathbb{R}$, $1 \leq i \leq n_1$. The magnetostatic problem is given by:

$$\begin{cases} \text{div } \mathbf{B}(x)=0, \\ \text{curl } (\mathbf{H}(x) - \mathbf{H}_s(x))=0, \end{cases} \tag{11}$$

with the following constitutive laws between the magnetic induction $\mathbf{B}$ and the magnetic field $\mathbf{H}$:

$$\mathbf{B}(x) = \mu(x)\,\mathbf{H}(x) \quad \forall x \in D. \tag{12}$$

Equations (11)-(12) are completed by the following boundary conditions:

$$\mathbf{B}(x) \cdot \mathbf{n}(x) = 0 \quad \text{on } \Gamma_D. \tag{13}$$

Now we introduce a scalar potential Ω [14] such that:

$$\mathbf{H}(x) = -\mathbf{grad}\ \Omega(x) + \mathbf{H}_s(x). \tag{14}$$

Then the problem (11)–(13) can be written as:

$$\left\{ \begin{array}{rcll} \text{div}\ (\mu(x)\mathbf{grad}\ \Omega(x)) & = & \text{div}\ (\mu(x)\mathbf{H}_s(x)) & \text{in } D, \\ \mu(x)\,(\mathbf{grad}\ \Omega(x) - \mathbf{H}_s(x)) \cdot \mathbf{n}(x) & = & 0 & \text{on } \Gamma_D. \end{array} \right. \tag{15}$$

The corresponding weak formulation takes the form:

Find $\Omega \in V_x$ *such that for all* $\lambda \in V_x$, *we have* :

$$\int_D \mu(x)\,\mathbf{grad}\ \Omega(x) \cdot \mathbf{grad}\ \lambda(x)\ dx = \int_D \mu(x)\,\mathbf{H}_s(x) \cdot \mathbf{grad}\ \lambda(x)\ dx. \tag{16}$$

Clearly, the solution of (16) is defined up to an additive constant and is not reachable in the general case. Consequently, we look for an approximation Ω^h of Ω belonging to the discrete space V_x^h:

Find $\Omega^h \in V_x^h$ *such that for all* $i,\ 1 \leq i \leq n_0,$ *we have* :

$$\int_D \mu(x)\,\mathbf{grad}\ \Omega^h(x) \cdot \mathbf{grad}\ w_{0i}(x)\ dx = \int_D \mu(x)\,\mathbf{H}_s(x) \cdot \mathbf{grad}\ w_{0i}(x)\ dx. \tag{17}$$

Once again, the solution of (17) is defined up to an additive constant. To ensure the uniqueness of the solution, a gauge condition has to be imposed (a value of the scalar potential at one point or its zero mean value on D can for example be prescribed). However, let us note that the corresponding magnetic fields

$$\mathbf{H} = -\mathbf{grad}\ \Omega + \mathbf{H}_s \quad \text{and} \quad \mathbf{H}^h = -\mathbf{grad}\ \Omega^h + \mathbf{H}_s,$$

as well as the corresponding magnetic flux densities

$$\mathbf{B} = \mu\,\mathbf{H} \quad \text{and} \quad \mathbf{B}^h = \mu\,\mathbf{H}^h$$

do not depend on this chosen gauge condition. Many *a posteriori* error estimations have been proposed in the literature to evaluate the error between $\mathbf{H}$, $\mathbf{B}$ and $\mathbf{H}^h$, $\mathbf{B}^h$ (see e.g. [3, 5, 8, 9, 24, 27]).

3.2. Stochastic magnetostatic problem

In this section, we are interested in a stochastic magnetostatic problem with uncertainties on the behavior law. The difference between the stochastic and the deterministic cases appears only on the permeability value, which is now supposed to be random. In the stochastic case, it is no longer a deterministic function of the spatial variable x, but it becomes a random field $\mu(x,\theta)$ where $\theta \in \Xi$ is an elementary event. We assume moreover that the permeability $\mu(x,\theta)$ can be explicitly expressed as a function of a random vector $\boldsymbol{\xi}$ (of independent random variables ξ_i) with a joint probability density function $f_{\boldsymbol{\xi}}$, and that for each realization of $\boldsymbol{\xi}$ the permeability μ is constant in each tetrahedral element T of the mesh $\mathcal{T}_h$. We also assume that there exist $\mu^0_{min} \in \mathbb{R}$ and $\mu^0_{max} \in \mathbb{R}$ such that:

$$0 < \mu^0_{min} < \mu_{min}(x) < \mu(x,\boldsymbol{\xi}) < \mu_{max}(x) < \mu^0_{max} \quad \forall\, \boldsymbol{\xi} \in \Theta^M,\ x \in D. \quad (18)$$

The equations modeling the stochastic problem are very similar to (11)–(13), except that the magnetic flux density, the magnetic field and the scalar potential become now random fields and are expressed as functions of x and $\boldsymbol{\xi}$, namely $\mathbf{B}(x,\boldsymbol{\xi})$, $\mathbf{H}(x,\boldsymbol{\xi})$ and $\Omega(x,\boldsymbol{\xi})$. The semi-weak formulation is given by:

Find $\Omega \in V_x \otimes V_{\boldsymbol{\xi}}$ such that for all $\boldsymbol{\xi} \in \Theta^M$ and $\lambda \in V_x$, we have:

$$\int_D \mu(x,\boldsymbol{\xi})\, \mathbf{grad}\ \Omega(x,\boldsymbol{\xi}) \cdot \mathbf{grad}\ \lambda(x)\, dx = \int_D \mu(x,\boldsymbol{\xi})\, \mathbf{H}_s(x) \cdot \mathbf{grad}\ \lambda(x)\, dx. \quad (19)$$

In the general case, the exact solution of (19) (defined up to an additive constant) can not be evaluated analytically. In the literature, some numerical methods have been proposed to approximate it [12, 13, 19, 20]. These methods consist in looking for an approximation $\Omega^{hi_0,P} \in V_x^{hi_0} \otimes V_{\boldsymbol{\xi}}^P$ of Ω such that:

$$\Omega^{hi_0,P}(x,\boldsymbol{\xi}) = \sum_{\boldsymbol{\alpha} \in K_P} \sum_{i=1, i\neq i_0}^{n_0} \Omega_{i\boldsymbol{\alpha}}\, w_{0i}(x) \Psi_{\boldsymbol{\alpha}}(\boldsymbol{\xi}), \quad (20)$$

where $\Psi_{\boldsymbol{\alpha}}$ is a polynomial chaos [15, 29] and $\Omega_{i\boldsymbol{\alpha}}$ are real coefficients to be determined. Let us denote that this choice of $\Omega^{hi_0,P}$ means that the value of $\Omega^{hi_0,P}$ at the node i_0 is equal to zero. Two kinds of methods allowing to determine $\Omega_{i\boldsymbol{\alpha}}$ can be considered, namely non intrusive ones and intrusive ones. Concerning the non intrusive methods (see [11, 13] and the references

therein), for a given $Q \in \mathbb{N}^*$ the coefficients $\Omega_{i\boldsymbol{\alpha}}$ are defined by:

$$\Omega_{i\boldsymbol{\alpha}} = \sum_{k=1}^{Q} \omega_k \; \Omega_i^h(\boldsymbol{\xi}_k) \; \Psi_{\boldsymbol{\alpha}}(\boldsymbol{\xi}_k). \tag{21}$$

The evaluation of coefficients $\Omega_{i\boldsymbol{\alpha}}$ in (21) requires Q evaluations of the scalar potential at node i: $\Omega_i^h(\boldsymbol{\xi}_k)$, $k = 1 : Q$ at special points $\boldsymbol{\xi}_k$. ω_k denotes the associated weight with the point $\boldsymbol{\xi}_k$. Consequently, Q deterministic problems corresponding to the cases of deterministic permeability $\mu(x, \boldsymbol{\xi}_k)$ have to be solved.

Concerning the intrusive method (SSFEM method, see [12, 19, 20]), the coefficients $\Omega_{i\boldsymbol{\alpha}}$ are determined by using the Galerkin projection:

$$\begin{aligned} & \mathrm{E}\left[\int_D \mu(x,\boldsymbol{\xi})\, \mathbf{grad}\; \Omega^{hi_0,P}(x,\boldsymbol{\xi}) \cdot \mathbf{grad}\; w_{0i}(x)\, dx\; \Psi_{\boldsymbol{\alpha}}(\boldsymbol{\xi})\right] \\ = \;& \mathrm{E}\left[\int_D \mu(x,\boldsymbol{\xi})\, \mathbf{H}_s(x) \cdot \mathbf{grad}\; w_{0i}(x)\, dx\; \Psi_{\boldsymbol{\alpha}}(\boldsymbol{\xi})\right], \end{aligned} \tag{22}$$

with $i = 1 : n_0 \backslash\, i_0$, $\boldsymbol{\alpha} \in K_P$. Equation (22) leads to a linear system of dimension $(n_0 - 1) \times P_{out}$ where P_{out} is the cardinality of K_P and the solution is the set of the coefficients $\Omega_{k\boldsymbol{\alpha}_i}$:

$$\begin{bmatrix} [\mathrm{E}\left[\Psi_{\boldsymbol{\alpha}_1}(\boldsymbol{\xi})\Psi_{\boldsymbol{\alpha}_1}(\boldsymbol{\xi})\boldsymbol{\Lambda}(\boldsymbol{\xi})\right]] & \cdots & \left[\mathrm{E}\left[\Psi_{\boldsymbol{\alpha}_1}(\boldsymbol{\xi})\Psi_{\boldsymbol{\alpha}_{P_{out}}}(\boldsymbol{\xi})\boldsymbol{\Lambda}(\boldsymbol{\xi})\right]\right] \\ \vdots & \ddots & \vdots \\ \left[\mathrm{E}[\Psi_{\boldsymbol{\alpha}_{P_{out}}}(\boldsymbol{\xi})\Psi_{\boldsymbol{\alpha}_1}(\boldsymbol{\xi})\boldsymbol{\Lambda}(\boldsymbol{\xi})]\right] & \cdots & \left[\mathrm{E}[\Psi_{\boldsymbol{\alpha}_{P_{out}}}(\boldsymbol{\xi})\Psi_{\boldsymbol{\alpha}_{P_{out}}}(\boldsymbol{\xi})\boldsymbol{\Lambda}(\boldsymbol{\xi})]\right] \end{bmatrix} \begin{bmatrix} [\Omega_{\boldsymbol{\alpha}_1}] \\ \vdots \\ \left[\Omega_{\boldsymbol{\alpha}_{P_{out}}}\right] \end{bmatrix}$$

$$= \begin{bmatrix} [\mathrm{E}[\boldsymbol{\beta}(\boldsymbol{\xi})\Psi_1(\boldsymbol{\xi})]] \\ \vdots \\ [\mathrm{E}[\boldsymbol{\beta}(\boldsymbol{\xi})\Psi_{P_{out}}(\boldsymbol{\xi})]] \end{bmatrix}. \tag{23}$$

The matrix $\boldsymbol{\Lambda}(\boldsymbol{\xi})$, the vector $\boldsymbol{\beta}(\boldsymbol{\xi})$ and the vector $\Omega_{\boldsymbol{\alpha}_i}$, $i = 1 : P_{out}$ are written in the following form:

$$[\boldsymbol{\Lambda}(\boldsymbol{\xi})]_{kl} = \int_D \mu(x,\boldsymbol{\xi})\, \mathbf{grad}\; w_{0k}(x) \cdot \mathbf{grad}\; w_{0l}(x)\, dx, \tag{24}$$

$$[\boldsymbol{\beta}(\boldsymbol{\xi})]_l = \int_D \mu(x,\boldsymbol{\xi}) \mathbf{H}_s(x) \cdot \mathbf{grad}\; w_{0l}(x)\, dx, \tag{25}$$

$$[\Omega_{\boldsymbol{\alpha}_i}]_k = \Omega_{k\boldsymbol{\alpha}_i}, \tag{26}$$

with $k = 1 : n_0,\ k \neq i_0$, $l = 1 : n_0,\ l \neq i_0$.

In the following section, we propose a residual based *a posteriori* error estimator which allows us to estimate the error between the solution Ω of (19) and its approximation $\Omega^{hi_0,P}$ given by (20) .

4. Error estimation

4.1. Definition of the errors

We first introduce Ω^{hi_0} such that

$$\int_D \mu(x,\boldsymbol{\xi})\,\mathbf{grad}\ \Omega^{hi_0}(x,\boldsymbol{\xi})\cdot\mathbf{grad}\ w_{0i}(x)\,dx = \int_D \mu(x,\boldsymbol{\xi})\,\mathbf{H}_s(x)\cdot\mathbf{grad}\ w_{0i}\,dx \tag{27}$$

$\forall i = 1 : n_0,\ i \neq i_0$, $\forall \boldsymbol{\xi} \in \Theta^M$, where $\Omega^{hi_0} \in V_x^{hi_0} \otimes V_{\boldsymbol{\xi}}$ is given by:

$$\Omega^{hi_0}(x,\boldsymbol{\xi}) = \sum_{i=1, i\neq i_0}^{n_0} \Omega_i(\boldsymbol{\xi})\, w_{0i}(x). \tag{28}$$

The field $\Omega^{hi_0}(x,\boldsymbol{\xi})$ is not explicitly available because the terms Ω_i are not real coefficients any more but unknown function of random variables. In this section, we first consider the error between $\Omega^{hi_0,P}$ given by (20) and Ω^{hi_0} given by (27)–(28), namely the stochastic error, which is defined by:

$$e^2_{sto}(\boldsymbol{\xi}) = \int_D \mu(x,\boldsymbol{\xi})\,|\mathbf{grad}\ \varepsilon_{sto}(x,\boldsymbol{\xi})|^2\ dx, \tag{29}$$

with

$$\varepsilon_{sto}(x,\boldsymbol{\xi}) = \Omega^{hi_0,P}(x,\boldsymbol{\xi}) - \Omega^{hi_0}(x,\boldsymbol{\xi}). \tag{30}$$

Then, we consider the error between $\Omega^{hi_0,P}$ and Ω, namely the global error, given by:

$$e^2_{glo}(\boldsymbol{\xi}) = \int_D \mu(x,\boldsymbol{\xi})\,|\mathbf{grad}\ \varepsilon_{glo}(x,\boldsymbol{\xi})|^2\ dx, \tag{31}$$

with

$$\varepsilon_{glo}(x,\boldsymbol{\xi}) = \Omega^{hi_0,P}(x,\boldsymbol{\xi}) - \Omega(x,\boldsymbol{\xi}). \tag{32}$$

We denote $\Omega^0 \in V_x^0 \otimes V_{\boldsymbol{\xi}}$ such that for all $\lambda \in V_x$ and $\boldsymbol{\xi} \in \Theta^M$ we have:

$$\int_D \mu(x,\boldsymbol{\xi})\,\mathbf{grad}\ \Omega^0(x,\boldsymbol{\xi})\cdot\mathbf{grad}\ \lambda(x)\,dx = \int_D \mu(x,\boldsymbol{\xi})\,\mathbf{H}_s(x)\cdot\mathbf{grad}\ \lambda(x)\,dx. \tag{33}$$

Similarly, we denote $\Omega^{h0} \in V_x^{h0} \otimes V_{\boldsymbol{\xi}}$ such that for all $i = 1 : n_0$ and $\boldsymbol{\xi} \in \Theta^M$ we have:

$$\int_D \mu(x,\boldsymbol{\xi})\, \mathbf{grad}\, \Omega^{h0}(x,\boldsymbol{\xi}) \cdot \mathbf{grad}\, w_{0i}(x)\, dx = \int_D \mu(x,\boldsymbol{\xi})\, \mathbf{H}_s(x) \cdot \mathbf{grad}\, w_{0i}(x)\, dx. \tag{34}$$

The existence and uniqueness of Ω^0 and Ω^{h0} have been proved in [26]. Since Ω^0 and Ω are equal up to an additive constant, they lead to the same magnetic field: $\mathbf{grad}\, \Omega^0(x,\boldsymbol{\xi}) = \mathbf{grad}\, \Omega(x,\boldsymbol{\xi})$. For the same reason, Ω^{h_0} and Ω^{hi_0} lead also to the same magnetic field. We also introduce $\Omega^{h0,P} \in V_x^{h_0} \otimes V_{\boldsymbol{\xi}}^P$ defined by:

$$\Omega^{h0,P}(x,\boldsymbol{\xi}) = \Omega^{hi_0,P}(x,\boldsymbol{\xi}) - \frac{1}{|D|} \int_D \Omega^{hi_0,P}(x,\boldsymbol{\xi})\, dx. \tag{35}$$

Clearly, we have:

$$e_{sto}^2(\boldsymbol{\xi}) = \int_D \mu(x,\boldsymbol{\xi})\, |\mathbf{grad}\, \varepsilon'_{sto}(x,\boldsymbol{\xi})|^2\, dx \tag{36}$$

and

$$e_{glo}^2(\boldsymbol{\xi}) = \int_D \mu(x,\boldsymbol{\xi})\, |\mathbf{grad}\, \varepsilon'_{glo}(x,\boldsymbol{\xi})|^2\, dx, \tag{37}$$

where

$$\varepsilon'_{sto}(x,\boldsymbol{\xi}) = \Omega^{h0,P}(x,\boldsymbol{\xi}) - \Omega^{h0}(x,\boldsymbol{\xi}) \tag{38}$$

and

$$\varepsilon'_{glo}(x,\boldsymbol{\xi}) = \Omega^{h0,P}(x,\boldsymbol{\xi}) - \Omega^{0}(x,\boldsymbol{\xi}). \tag{39}$$

4.2. Stochastic error estimator

Definition 1. *The stochastic estimator η_{sto} is defined by:*

$$\eta_{sto}^2(\boldsymbol{\xi}) = \mathbf{r}^t(\boldsymbol{\xi}) \boldsymbol{\Lambda}_0^{-1} \mathbf{r}(\boldsymbol{\xi}), \tag{40}$$

where $\mathbf{r}(\boldsymbol{\xi})$ is the residual vector term given by:

$$[\mathbf{r}(\boldsymbol{\xi})]_i = \int_D \mu(x,\boldsymbol{\xi}) \mathbf{grad}\, \Omega^{hi_0,P}(x,\boldsymbol{\xi}) \cdot \mathbf{grad}\, w_{0i}(x)\, dx - \int_D \mu(x,\boldsymbol{\xi}) \mathbf{H}_s(x) \cdot \mathbf{grad}\, w_{0i}(x)\, dx \tag{41}$$

for all $1 \leq i \leq n_0,\ i \neq i_0$, and $\boldsymbol{\Lambda}_0$ is the mean value of the stiffness matrix:

$$\boldsymbol{\Lambda}_0 = \mathrm{E}[\boldsymbol{\Lambda}(\boldsymbol{\xi})], \tag{42}$$

with $\boldsymbol{\Lambda}$ defined in (24).

The purpose of this subsection (see Theorem 1 below) is to prove the equivalence between the stochastic error (29) and the estimator (40). In order to do it, two lemmas are first established.

Lemma 1. *The stochastic error e_{sto} defined in (29) can be written in the following form:*

$$e_{sto}^2(\boldsymbol{\xi}) = \mathbf{r}^t(\boldsymbol{\xi})\boldsymbol{\Lambda}^{-1}(\boldsymbol{\xi})\mathbf{r}(\boldsymbol{\xi}). \tag{43}$$

Proof. Let us define the vector $\boldsymbol{\varepsilon}(\boldsymbol{\xi})$ such that

$$[\boldsymbol{\varepsilon}(\boldsymbol{\xi})]_i = \varepsilon_i(\boldsymbol{\xi}), \quad i = 1 : n_0,\ i \neq i_0, \tag{44}$$

where

$$\varepsilon_i(\boldsymbol{\xi}) = \sum_{\boldsymbol{\alpha} \in K_P} \Omega_{i\boldsymbol{\alpha}} \Psi_{\boldsymbol{\alpha}}(\boldsymbol{\xi}) - \Omega_i(\boldsymbol{\xi}), \tag{45}$$

with $\Omega_{i\boldsymbol{\alpha}}$ defined in (20) and Ω_i defined in (28). From the definitions (24) of $\boldsymbol{\Lambda}(\boldsymbol{\xi})$ and (44) of $\boldsymbol{\varepsilon}(\boldsymbol{\xi})$, the definitions (20) of $\Omega^{hi_0,P}$ and (28) of Ω^{hi_0}, as well as the weak formulation (27) associated to the definition (41) of $\mathbf{r}(\boldsymbol{\xi})$, we obtain:

$$\boldsymbol{\Lambda}(\boldsymbol{\xi})\boldsymbol{\varepsilon}(\boldsymbol{\xi}) = \mathbf{r}(\boldsymbol{\xi}). \tag{46}$$

Then, substituting (20) and (28) in (29) and using the definitions (45) and (24), we have:

$$e_{sto}^2(\boldsymbol{\xi}) = \boldsymbol{\varepsilon}^t(\boldsymbol{\xi})\boldsymbol{\Lambda}(\boldsymbol{\xi})\boldsymbol{\varepsilon}(\boldsymbol{\xi}). \tag{47}$$

(43) is a direct consequence of (46) and (47). □

Lemma 2. *Let us denote $\boldsymbol{\Lambda}_1(\boldsymbol{\xi})$ and $\boldsymbol{\Lambda}_2(\boldsymbol{\xi})$ the two matrices of dimension $(n_0 - 1) \times (n_0 - 1)$ such that:*

$$[\boldsymbol{\Lambda}_1]_{ij}(\boldsymbol{\xi}) = \int_D \mu_1(x, \boldsymbol{\xi}) \mathbf{grad}\ \ w_{0i}(x) \cdot \mathbf{grad}\ \ w_{0j}(x)\, dx,$$

$$[\boldsymbol{\Lambda}_2]_{ij}(\boldsymbol{\xi}) = \int_D \mu_2(x, \boldsymbol{\xi}) \mathbf{grad}\ \ w_{0i}(x) \cdot \mathbf{grad}\ \ w_{0j}(x)\, dx,$$

with $1 \leq i \leq n_0,\ i \neq i_0,\ 1 \leq j \leq n_0,\ j \neq i_0$ and $0 < \mu_1(x, \boldsymbol{\xi}) \leq \mu_2(x, \boldsymbol{\xi})$ for all $x \in D$, and $\boldsymbol{\xi} \in \Theta^M$. Then we have:

$$\mathbf{r}^t(\boldsymbol{\xi})\boldsymbol{\Lambda}_2^{-1}(\boldsymbol{\xi})\mathbf{r}(\boldsymbol{\xi}) \leq \mathbf{r}^t(\boldsymbol{\xi})\boldsymbol{\Lambda}_1^{-1}(\boldsymbol{\xi})\mathbf{r}(\boldsymbol{\xi}),\ \forall \boldsymbol{\xi} \in \Theta^M. \tag{48}$$

Proof. Let us denote

$$\boldsymbol{\varepsilon}_2(\boldsymbol{\xi}) = \boldsymbol{\Lambda}_2^{-1}(\boldsymbol{\xi})\mathbf{r}(\boldsymbol{\xi}), \tag{49}$$

$$\boldsymbol{\Lambda}_3(\boldsymbol{\xi}) = \boldsymbol{\Lambda}_2(\boldsymbol{\xi}) - \boldsymbol{\Lambda}_1(\boldsymbol{\xi}). \tag{50}$$

First,

$$\mathbf{r}^t(\boldsymbol{\xi})\boldsymbol{\Lambda}_2^{-1}(\boldsymbol{\xi})\mathbf{r}(\boldsymbol{\xi}) \;\; = \;\; \boldsymbol{\varepsilon}_2^t(\boldsymbol{\xi})\boldsymbol{\Lambda}_2(\boldsymbol{\xi})\boldsymbol{\varepsilon}_2(\boldsymbol{\xi}). \tag{51}$$

Since

$$\mathbf{r}^t(\boldsymbol{\xi})\boldsymbol{\Lambda}_1^{-1}(\boldsymbol{\xi})\mathbf{r}(\boldsymbol{\xi}) = \boldsymbol{\varepsilon}_2^t(\boldsymbol{\xi})\boldsymbol{\Lambda}_2^t(\boldsymbol{\xi})\boldsymbol{\Lambda}_1^{-1}(\boldsymbol{\xi})\boldsymbol{\Lambda}_2(\boldsymbol{\xi})\boldsymbol{\varepsilon}_2(\boldsymbol{\xi}), \tag{52}$$

we have:

$$\begin{aligned}
&\mathbf{r}^t(\boldsymbol{\xi})\boldsymbol{\Lambda}_1^{-1}(\boldsymbol{\xi})\mathbf{r}(\boldsymbol{\xi}) = \boldsymbol{\varepsilon}_2^t(\boldsymbol{\xi})(\boldsymbol{\Lambda}_1^t(\boldsymbol{\xi}) + \boldsymbol{\Lambda}_3^t(\boldsymbol{\xi}))\boldsymbol{\Lambda}_1^{-1}(\boldsymbol{\xi})(\boldsymbol{\Lambda}_1(\boldsymbol{\xi}) + \boldsymbol{\Lambda}_3(\boldsymbol{\xi}))\boldsymbol{\varepsilon}_2(\boldsymbol{\xi}) \\
&= \boldsymbol{\varepsilon}_2^t(\boldsymbol{\xi})\boldsymbol{\Lambda}_1(\boldsymbol{\xi})\boldsymbol{\varepsilon}_2(\boldsymbol{\xi}) + 2\boldsymbol{\varepsilon}_2^t(\boldsymbol{\xi})\boldsymbol{\Lambda}_3(\boldsymbol{\xi})\boldsymbol{\varepsilon}_2(\boldsymbol{\xi}) + \boldsymbol{\varepsilon}_2^t(\boldsymbol{\xi})\boldsymbol{\Lambda}_3^t(\boldsymbol{\xi})\boldsymbol{\Lambda}_1^{-1}(\boldsymbol{\xi})\boldsymbol{\Lambda}_3(\boldsymbol{\xi})\boldsymbol{\varepsilon}_2(\boldsymbol{\xi}) \\
&= \boldsymbol{\varepsilon}_2^t(\boldsymbol{\xi})\boldsymbol{\Lambda}_2(\boldsymbol{\xi})\boldsymbol{\varepsilon}_2(\boldsymbol{\xi}) + \boldsymbol{\varepsilon}_2^t(\boldsymbol{\xi})\boldsymbol{\Lambda}_3(\boldsymbol{\xi})\boldsymbol{\varepsilon}_2(\boldsymbol{\xi}) + \boldsymbol{\varepsilon}_2^t(\boldsymbol{\xi})\boldsymbol{\Lambda}_3^t(\boldsymbol{\xi})\boldsymbol{\Lambda}_1^{-1}(\boldsymbol{\xi})\boldsymbol{\Lambda}_3(\boldsymbol{\xi})\boldsymbol{\varepsilon}_2(\boldsymbol{\xi}) \\
&= \mathbf{r}^t(\boldsymbol{\xi})\boldsymbol{\Lambda}_2^{-1}(\boldsymbol{\xi})\mathbf{r}(\boldsymbol{\xi}) + \boldsymbol{\varepsilon}_2^t(\boldsymbol{\xi})\boldsymbol{\Lambda}_3(\boldsymbol{\xi})\boldsymbol{\varepsilon}_2(\boldsymbol{\xi}) + \boldsymbol{\varepsilon}_2^t(\boldsymbol{\xi})\boldsymbol{\Lambda}_3^t(\boldsymbol{\xi})\boldsymbol{\Lambda}_1^{-1}(\boldsymbol{\xi})\boldsymbol{\Lambda}_3(\boldsymbol{\xi})\boldsymbol{\varepsilon}_2(\boldsymbol{\xi}).
\end{aligned} \tag{53}$$

(48) is deduced from (53), due to the facts that the matrix $\boldsymbol{\Lambda}_1^{-1}$ and the matrix $\boldsymbol{\Lambda}_3$ are semi positive definite. □

Theorem 1. *Let us denote*

$$k_2 = \max_{x\in D}\left(\frac{\mathrm{E}[\mu(x,\boldsymbol{\xi})]}{\mu_{\min}(x)}\right) \tag{54}$$

and

$$k_1 = \min_{x\in D}\left(\frac{\mathrm{E}[\mu(x,\boldsymbol{\xi})]}{\mu_{\max}(x)}\right). \tag{55}$$

Then,

$$k_1\ \eta_{sto}^2(\boldsymbol{\xi}) \leqslant e_{sto}^2(\boldsymbol{\xi}) \leqslant k_2\ \eta_{sto}^2(\boldsymbol{\xi}). \tag{56}$$

Proof. (56) is deduced by using Lemma 1, Lemma 2 and the definition of $\boldsymbol{\Lambda_0}$ in (42). □

Here, one can notice that the coefficients k_1 and k_2 can be evaluated explicitly. In practice, the ratio k_2/k_1 is in the order of some units. Then, the ratio between the upper bound and the lower bound of the stochastic error is also in the order of some units. Furthermore, the estimation (56) does not depend on the choice of the stochastic approximation basis (even if the polynomial chaos are used in this paper to illustrate the approach) and on the uncertainties propagation method (non intrusive or intrusive one). It can also be used for the case of wavelet decomposition for example [21]. However, the error estimator requires the computation of the term $\mathbf{r}^t(\boldsymbol{\xi})\boldsymbol{\Lambda}_0^{-1}\mathbf{r}(\boldsymbol{\xi})$ that might be numerically expansive. By the way, as the matrix $\boldsymbol{\Lambda}_0$ is deterministic, some techniques can be used to calculate this term (triangular decomposition of $\boldsymbol{\Lambda}_0$ if the memory system allows the storage of the triangular matrices, or performing a super pre-conditioning on the matrix $\boldsymbol{\Lambda}_0$).

We are now interested in estimating the global error defined by (37). In the following of the paper, the constant C denotes to a generic constant independent on the mesh $\mathcal{T}_h$, on the exact solution $\Omega(x,\boldsymbol{\xi})$, and on the degree of the polynomial chaos P.

4.3. Reliability of the global error estimator

Definition 2. *The global estimator η_{glo} is defined by:*

$$\eta_{glo}(\boldsymbol{\xi}) = \sqrt{\frac{1}{\mu^0_{\min}}}\left(\sum_{F\in\Delta_{in}}\int_F h_F\left[\mu(x,\boldsymbol{\xi})(\mathbf{grad}\ \Omega^{hi_0,P}(x,\boldsymbol{\xi})-\mathbf{H}_s(x))\right]_F^2\,ds + \sum_{F\in\Delta_{\mathbf{B}}}\int_F h_F\left|\mu(x,\boldsymbol{\xi})(\mathbf{grad}\ \Omega^{hi_0,P}(x,\boldsymbol{\xi})-\mathbf{H}_s(x))\cdot\mathbf{n}(x)\right|^2 ds\right)^{\frac{1}{2}} + \sqrt{k_2\frac{\mu^0_{\max}}{\mu^0_{\min}}}\,\eta_{sto}(\boldsymbol{\xi}), \tag{57}$$

where $\left[\mu(x,\boldsymbol{\xi})(\mathbf{grad}\ \Omega^{hi_0,P}(x,\boldsymbol{\xi})-\mathbf{H}_s(x))\right]_F$ denotes the jump of the normal component of $\mu(x,\boldsymbol{\xi})(\mathbf{grad}\ \Omega^{hi_0,P}(x,\boldsymbol{\xi})-\mathbf{H}_s(x))$ through the facet F, and Δ_{in} and $\Delta_{\mathbf{B}}$ are the set of facets respectively located inside the domain D and on the boundary of the domain Γ_D.

The purpose of this section (see Theorem 2 below) is to prove the reliability of the estimator (57). In order to do it, five lemmas are first established.

Lemma 3. *Let us denote* $\Pi\boldsymbol{\varepsilon}'(x,\boldsymbol{\xi}) \in V_x^h$ *the Scott-Zhang interpolation of* $\boldsymbol{\varepsilon}'_{glo}(x,\boldsymbol{\xi}) \in V_x$ *[25] defined in (39):*

$$\Pi\boldsymbol{\varepsilon}'_{glo}(x,\boldsymbol{\xi}) = \sum_{i=1}^{n_0} a_i(\boldsymbol{\xi}) w_{0i}(x), \tag{58}$$

where the dependency of $a_i(\boldsymbol{\xi})$ *in* $\boldsymbol{\varepsilon}'_{glo}(x,\boldsymbol{\xi})$ *is described in section 2 of [25]. Then we have :*

$$e^2_{glo}(\boldsymbol{\xi}) = E_{glo1}(\boldsymbol{\xi}) + E_{glo2}(\boldsymbol{\xi}), \tag{59}$$

where:

$$\begin{aligned} E_{glo1}(\boldsymbol{\xi}) &= \int_D \mu(x,\boldsymbol{\xi}) \mathbf{grad}\ \Omega^{h0,P}(x,\boldsymbol{\xi}) \cdot \mathbf{grad}\ (\boldsymbol{\varepsilon}'_{glo}(x,\boldsymbol{\xi}) - \Pi\boldsymbol{\varepsilon}'_{glo}(x,\boldsymbol{\xi}))\, dx \\ &\quad - \int_D \mu(x,\boldsymbol{\xi}) \mathbf{H}_s(x) \cdot \mathbf{grad}\ (\boldsymbol{\varepsilon}'_{glo}(x,\boldsymbol{\xi}) - \Pi\boldsymbol{\varepsilon}'_{glo}(x,\boldsymbol{\xi}))\, dx, \end{aligned} \tag{60}$$

and

$$E_{glo2}(\boldsymbol{\xi}) = \int_D \mu(x,\boldsymbol{\xi}) \mathbf{grad}\ (\Omega^{h0,P}(x,\boldsymbol{\xi}) - \Omega^{h0}(x,\boldsymbol{\xi})) \cdot \mathbf{grad}\ \Pi\boldsymbol{\varepsilon}'_{glo}(x,\boldsymbol{\xi})\, dx. \tag{61}$$

Proof. From the definitions (37), (39) and the formulation (33) we have:

$$\begin{aligned} e^2_{glo}(\boldsymbol{\xi}) &= \int_D \mu(x,\boldsymbol{\xi}) \mathbf{grad}\ \Omega^{h0,P}(x,\boldsymbol{\xi}) \cdot \mathbf{grad}\ \boldsymbol{\varepsilon}'_{glo}(x,\boldsymbol{\xi})\, dx \\ &\quad - \int_D \mu(x,\boldsymbol{\xi}) \mathbf{H}_s(x) \cdot \mathbf{grad}\ \boldsymbol{\varepsilon}'_{glo}(x,\boldsymbol{\xi})\, dx. \end{aligned} \tag{62}$$

Since $\Pi\boldsymbol{\varepsilon}'_{glo}(x,\boldsymbol{\xi}) \in V_x^h$, from (34) we can deduce that:

$$\begin{aligned} &\int_D \mu(x,\boldsymbol{\xi}) \mathbf{grad}\ \Omega^{h0}(x,\boldsymbol{\xi}) \cdot \mathbf{grad}\ \Pi\boldsymbol{\varepsilon}'_{glo}(x,\boldsymbol{\xi})\, dx \\ &\quad = \int_D \mu(x,\boldsymbol{\xi}) \mathbf{H}_s(x) \cdot \mathbf{grad}\ \Pi\boldsymbol{\varepsilon}'_{glo}(x,\boldsymbol{\xi})\, dx. \end{aligned} \tag{63}$$

(59) is deduced from (62) and (63). □

Lemma 4. *We have:*

$$\int_D \mu(x,\boldsymbol{\xi})|\mathbf{grad}\ \Pi\boldsymbol{\varepsilon}'_{glo}(x,\boldsymbol{\xi})|^2\,dx \leq C\frac{\mu^0_{\max}}{\mu^0_{\min}}\int_D \mu(x,\boldsymbol{\xi})|\mathbf{grad}\ \boldsymbol{\varepsilon}'_{glo}(x,\boldsymbol{\xi})|^2\,dx. \tag{64}$$

Proof. From corollary 4.1 in [25] with $l = m = 1$, $p = 2$ we can deduce that:

$$\int_D |\mathbf{grad}\,\Pi\boldsymbol{\varepsilon}'_{glo}(x,\boldsymbol{\xi})|^2\,dx \leq C\left(\int_D |\mathbf{grad}\ \boldsymbol{\varepsilon}'_{glo}(x,\boldsymbol{\xi})|^2\,dx + \int_D |\boldsymbol{\varepsilon}'_{glo}(x,\boldsymbol{\xi})|^2\,dx\right). \tag{65}$$

We can notice that

$$\int_D \boldsymbol{\varepsilon}'_{glo}(x,\boldsymbol{\xi})\,dx = \int_D (\Omega^{h0,P}(x,\boldsymbol{\xi}) - \Omega^0(x,\boldsymbol{\xi}))\,dx = 0. \tag{66}$$

Then, applying the Poincaré inequality we have:

$$\int_D |\boldsymbol{\varepsilon}'_{glo}(x,\boldsymbol{\xi})|^2\,dx \leq C\int_D |\mathbf{grad}\ \boldsymbol{\varepsilon}'_{glo}(x,\boldsymbol{\xi})|^2\,dx. \tag{67}$$

From (65), (67) and (18), (64) is established. □

Lemma 5.

$$\begin{aligned}\sum_{F\in\Delta}\int_F h_F^{-1}|\boldsymbol{\varepsilon}'_{glo}(x,\boldsymbol{\xi}) - \Pi\boldsymbol{\varepsilon}'_{glo}(x,\boldsymbol{\xi})|^2\,ds \\ + \sum_{T\in T_{\mathcal{T}_h}}\int_T h_T^{-2}|\boldsymbol{\varepsilon}'_{glo}(x,\boldsymbol{\xi}) - \Pi\boldsymbol{\varepsilon}'_{glo}(x,\boldsymbol{\xi})|^2\,dx \\ \leq C\int_D |\mathbf{grad}\ \boldsymbol{\varepsilon}'_{glo}(x,\boldsymbol{\xi})|^2\,dx,\end{aligned} \tag{68}$$

where Δ and $T_{\mathcal{T}_h}$ are respectively the set of facets and elements of the mesh $\mathcal{T}_h$ and h_F, h_T are respectively the diameters of circumscribed circle of the facet F and of circumscribed sphere of the element T.

Proof. From corollary 4.1 in [25] with $l = 1$, $m = 0$, $p = 2$, and using (67) we can deduce that:

$$\sum_{T\in T_{\mathcal{T}_h}}\int_T h_T^{-2}|\boldsymbol{\varepsilon}'_{glo}(x,\boldsymbol{\xi}) - \Pi\boldsymbol{\varepsilon}'_{glo}(x,\boldsymbol{\xi})|^2\,dx \leq C\int_D |\mathbf{grad}\ \boldsymbol{\varepsilon}'_{glo}(x,\boldsymbol{\xi})|^2\,dx. \tag{69}$$

By using Lemma 4 in [25] we have:

$$
\begin{aligned}
& h_T \int_{F_T} |\boldsymbol{\varepsilon}'_{glo}(x,\boldsymbol{\xi}) - \Pi\boldsymbol{\varepsilon}'_{glo}(x,\boldsymbol{\xi})|^2 \, ds \\
\leq \;& C\Big(\int_T |\boldsymbol{\varepsilon}'_{glo}(x,\boldsymbol{\xi}) - \Pi\boldsymbol{\varepsilon}'_{glo}(x,\boldsymbol{\xi})|^2 \, dx \\
& + h_T^2 \int_T |\mathbf{grad}\ (\boldsymbol{\varepsilon}'_{glo}(x,\boldsymbol{\xi}) - \Pi\boldsymbol{\varepsilon}'_{glo}(x,\boldsymbol{\xi}))|^2 \, dx \Big),
\end{aligned} \tag{70}
$$

where F_T is the set of the four facets belonging to the element T. By using (69) and (70) we obtain:

$$
\begin{aligned}
& \sum_{T \in T_{\mathcal{T}_h}} h_T^{-1} \int_{F_T} |\boldsymbol{\varepsilon}'_{glo}(x,\boldsymbol{\xi}) - \Pi\boldsymbol{\varepsilon}'_{glo}(x,\boldsymbol{\xi})|^2 \, ds \\
& + \sum_{T \in T_{\mathcal{T}_h}} h_T^{-2} \int_T |\boldsymbol{\varepsilon}'_{glo}(x,\boldsymbol{\xi}) - \Pi\boldsymbol{\varepsilon}'_{glo}(x,\boldsymbol{\xi})|^2 \, dx \\
\leq \;& C \int_D |\mathbf{grad}\ \boldsymbol{\varepsilon}'_{glo}(x,\boldsymbol{\xi})|^2 \, dx.
\end{aligned} \tag{71}
$$

Inequality (68) is deduced from (71) by the fact that $h_T \sim h_F$, using the regularity of the mesh $\mathcal{T}_h$. □

Lemma 6.

$$
\begin{aligned}
& E_{glo1}(\boldsymbol{\xi}) \leq \\
& C\, e_{glo}(\boldsymbol{\xi}) \sqrt{\frac{1}{\mu^0_{\min}}} \Big(\sum_{F \in \Delta_{in}} \int_F h_F \left[\mu(x,\boldsymbol{\xi})(\mathbf{grad}\ \Omega^{h0,P}(x,\boldsymbol{\xi}) - \mathbf{H}_s(x)) \right]_F^2 \, ds \\
& + \sum_{F \in \Delta_{\mathbf{B}}} \int_F h_F \left| \mu(x,\boldsymbol{\xi})(\mathbf{grad}\ \Omega^{h0,P}(x,\boldsymbol{\xi}) - \mathbf{H}_s(x)) \cdot \mathbf{n}(x) \right|^2 \, ds \Big)^{\frac{1}{2}}.
\end{aligned} \tag{72}
$$

Proof. By applying the Green formula, we obtain:

$$E_{glo1}(\boldsymbol{\xi}) =$$

$$\sum_{T\in T_{\mathcal{T}_h}} \int_{F_T} \mu(x,\boldsymbol{\xi})(\mathbf{grad}\ \Omega^{h0,P}(x,\boldsymbol{\xi}) - \mathbf{H}_s(x)) \cdot \mathbf{n}(x)(\boldsymbol{\varepsilon}'_{glo}(x,\boldsymbol{\xi}) - \Pi\boldsymbol{\varepsilon}'_{glo}(x,\boldsymbol{\xi}))\, ds$$

$$+ \sum_{T\in T_{\mathcal{T}_h}} \int_{T} \text{div}\ \left(\mu(x,\boldsymbol{\xi})(\mathbf{grad}\ \Omega^{h0,P}(x,\boldsymbol{\xi}) - \mathbf{H}_s(x))\right)(\boldsymbol{\varepsilon}'_{glo}(x,\boldsymbol{\xi}) - \Pi\boldsymbol{\varepsilon}'_{glo}(x,\boldsymbol{\xi}))\, dx. \tag{73}$$

By using the assumption that the permeability μ is constant in each element T of the mesh $\mathcal{T}_h$ and (10), we can deduce that:

$$\text{div}\ \left(\mu(x,\boldsymbol{\xi})(\mathbf{grad}\ \Omega^{h0,P}(x,\boldsymbol{\xi}) - \mathbf{H}_s(x))\right) = 0 \quad \forall x \in T. \tag{74}$$

By splitting the first term of the right hand-side of (73) on the facets in a boundary contribution and an inner contribution, we obtain:

$$E_{glo1}(\boldsymbol{\xi}) =$$

$$\sum_{F\in\Delta_{in}} \int_{F} \left[\mu(x,\boldsymbol{\xi})(\mathbf{grad}\ \Omega^{h0,P}(x,\boldsymbol{\xi}) - \mathbf{H}_s(x))\right]_F (\boldsymbol{\varepsilon}'_{glo}(x,\boldsymbol{\xi}) - \Pi\boldsymbol{\varepsilon}'_{glo}(x,\boldsymbol{\xi}))\, ds$$

$$+ \sum_{F\in\Delta_{\mathbf{B}}} \int_{F} \mu(x,\boldsymbol{\xi})(\mathbf{grad}\ \Omega^{h0,P}(x,\boldsymbol{\xi}) - \mathbf{H}_s(x)) \cdot \mathbf{n}(x)(\boldsymbol{\varepsilon}'_{glo}(x,\boldsymbol{\xi}) - \Pi\boldsymbol{\varepsilon}'_{glo}(x,\boldsymbol{\xi}))\, ds. \tag{75}$$

Consequently, we deduce from the Cauchy-Schwarz inequality that:

$$E_{glo1}(\boldsymbol{\xi}) \leq \left\{ \sum_{F\in\Delta} \int_{F} h_F^{-1} \left(\boldsymbol{\varepsilon}'_{glo}(x,\boldsymbol{\xi}) - \Pi\boldsymbol{\varepsilon}'_{glo}(x,\boldsymbol{\xi})\right)^2 ds \right\}^{\frac{1}{2}}$$

$$\times \left\{ \sum_{F\in\Delta_{in}} \int_{F} h_F \left[\mu(x,\boldsymbol{\xi})(\mathbf{grad}\ \Omega^{h0,P}(x,\boldsymbol{\xi}) - \mathbf{H}_s(x))\right]_F^2 ds \right. \tag{76}$$

$$\left. + \sum_{F\in\Delta_{\mathbf{B}}} \int_{F} h_F \left|\mu(x,\boldsymbol{\xi})(\mathbf{grad}\ \Omega^{h0,P}(x,\boldsymbol{\xi}) - \mathbf{H}_s(x)) \cdot \mathbf{n}(x)\right|^2 ds \right\}^{\frac{1}{2}}.$$

By using Lemma 5 we obtain:

$$E_{glo1}(\boldsymbol{\xi}) \leq C \left\{ \int_D |\mathbf{grad}\ \boldsymbol{\varepsilon}'_{glo}(x,\boldsymbol{\xi})|^2\, dx \right\}^{\frac{1}{2}}$$

$$\times \left\{ \sum_{F\in\Delta_{in}} \int_F h_F \left[\mu(x,\boldsymbol{\xi})(\mathbf{grad}\ \Omega^{h0,P}(x,\boldsymbol{\xi}) - \mathbf{H}_s(x))\right]_F^2\, ds \right. \tag{77}$$

$$\left. + \sum_{F\in\Delta_{\mathbf{B}}} \int_F h_F \left|\mu(x,\boldsymbol{\xi})(\mathbf{grad}\ \Omega^{h0,P}(x,\boldsymbol{\xi}) - \mathbf{H}_s(x))\cdot\mathbf{n}(x)\right|^2\, ds \right\}^{\frac{1}{2}}.$$

We can notice that:

$$\int_D \left|\mathbf{grad}\ \boldsymbol{\varepsilon}'_{glo}(x,\boldsymbol{\xi})\right|^2\, dx \leq \frac{1}{\mu^0_{\min}} \int_D \mu(x,\boldsymbol{\xi}) \left|\mathbf{grad}\ \boldsymbol{\varepsilon}'_{glo}(x,\boldsymbol{\xi})\right|^2\, dx, \tag{78}$$

so that we can deduce (72) from (77) and (78). □

Lemma 7. *We have:*

$$E_{glo2}(\boldsymbol{\xi}) \leq C\sqrt{\frac{\mu^0_{\max}}{\mu^0_{\min}}}\, e_{sto}(\boldsymbol{\xi}) e_{glo}(\boldsymbol{\xi}). \tag{79}$$

Proof. By using the Cauchy-Schwarz inequality, we obtain:

$$E_{glo2}(\boldsymbol{\xi}) = \int_D \mu(x,\boldsymbol{\xi})\mathbf{grad}\ (\Omega^{h0,P}(x,\boldsymbol{\xi}) - \Omega^{h0}(x,\boldsymbol{\xi}))\cdot\mathbf{grad}\ \Pi\boldsymbol{\varepsilon}'_{glo}(x,\boldsymbol{\xi})\, dx$$

$$= \int_D \mu(x,\boldsymbol{\xi})\mathbf{grad}\ \boldsymbol{\varepsilon}'_{sto}(x,\boldsymbol{\xi})\cdot\mathbf{grad}\ \Pi\boldsymbol{\varepsilon}'_{glo}(x,\boldsymbol{\xi})\, dx$$

$$\leq \left(\int_D \mu(x,\boldsymbol{\xi})|\mathbf{grad}\ \boldsymbol{\varepsilon}'_{sto}(x,\boldsymbol{\xi})|^2\, dx\right)^{\frac{1}{2}} \left(\int_D \mu(x,\boldsymbol{\xi})|\mathbf{grad}\ \Pi\boldsymbol{\varepsilon}'_{glo}(x,\boldsymbol{\xi})|^2\, dx\right)^{\frac{1}{2}}. \tag{80}$$

By using Lemma 4, we obtain:

$$\begin{aligned} E_{glo2}(\boldsymbol{\xi}) &\leq C\sqrt{\frac{\mu^0_{\max}}{\mu^0_{\min}}}\left(\int_D \mu(x,\boldsymbol{\xi})|\mathbf{grad}\ \boldsymbol{\varepsilon}'_{sto}(x,\boldsymbol{\xi})|^2\,dx\right)^{\frac{1}{2}} \\ &\quad\times\left(\int_D \mu(x,\boldsymbol{\xi})|\mathbf{grad}\ \boldsymbol{\varepsilon}'_{glo}(x,\boldsymbol{\xi})|^2\,dx\right)^{\frac{1}{2}} \qquad (81) \\ &= C\sqrt{\frac{\mu^0_{\max}}{\mu^0_{\min}}}\,e_{sto}(\boldsymbol{\xi})e_{glo}(\boldsymbol{\xi}). \end{aligned}$$

□

Theorem 2. *By defining $e^2_{glo}(\boldsymbol{\xi})$ in (37) and $\eta^2_{glo}(\boldsymbol{\xi})$ in (57) we have:*

$$e^2_{glo}(\boldsymbol{\xi}) \leq C\eta^2_{glo}(\boldsymbol{\xi}). \qquad (82)$$

Proof. From Lemmas 3, 6 and 7 one can deduce that

$$\begin{aligned} e_{glo}(\boldsymbol{\xi}) \leq C\sqrt{\frac{1}{\mu^0_{\min}}}\Bigg(&\sum_{F\in\Delta_{in}}\int_F h_F\left[\mu(x,\boldsymbol{\xi})(\mathbf{grad}\ \Omega^{h0,P}(x,\boldsymbol{\xi})-\mathbf{H}_s(x))\right]^2_F\,ds \\ &+\sum_{F\in\Delta_{\mathbf{B}}}\int_F h_F\left|\mu(x,\boldsymbol{\xi})(\mathbf{grad}\ \Omega^{h0,P}(x,\boldsymbol{\xi})-\mathbf{H}_s(x))\cdot\mathbf{n}(x)\right|^2\,ds\Bigg)^{\frac{1}{2}} \\ &+\sqrt{\frac{\mu^0_{\max}}{\mu^0_{\min}}}\,e_{sto}(\boldsymbol{\xi}). \end{aligned} \qquad (83)$$

By using Theorem 1, we can deduce

$$\begin{aligned} e_{glo}(\boldsymbol{\xi}) \leq C\sqrt{\frac{1}{\mu^0_{\min}}}\Bigg(&\sum_{F\in\Delta_{in}}\int_F h_F\left[\mu(x,\boldsymbol{\xi})(\mathbf{grad}\ \Omega^{h0,P}(x,\boldsymbol{\xi})-\mathbf{H}_s(x))\right]^2_F\,ds+ \\ &\sum_{F\in\Delta_{\mathbf{B}}}\int_F h_F\left|\mu(x,\boldsymbol{\xi})(\mathbf{grad}\ \Omega^{h0,P}(x,\boldsymbol{\xi})-\mathbf{H}_s(x))\cdot\mathbf{n}(x)\right|^2\,ds\Bigg)^{\frac{1}{2}} \\ &+\sqrt{k_2\frac{\mu^0_{\max}}{\mu^0_{\min}}}\,\eta_{sto}(\boldsymbol{\xi}). \end{aligned} \qquad (84)$$

Then, (82) is deduced by using the definition (57), due the fact that $\mathbf{grad}\ \Omega^{hi_0,P}(x,\boldsymbol{\xi}) = \mathbf{grad}\ \Omega^{h0,P}(x,\boldsymbol{\xi})$. □

One can notice that the global error estimator η^2_{glo} defined in (57) can be divided in two parts. The first part related to

$$\begin{aligned}\eta^2_{spa}(\boldsymbol{\xi}) &= \sum_{F\in\Delta_{in}} \int_F h_F \left[\mu(x,\boldsymbol{\xi})(\mathbf{grad}\ \Omega^{hi_0,P}(x,\boldsymbol{\xi}) - \mathbf{H}_s(x))\right]^2_F\, ds \\ &\quad + \sum_{F\in\Delta_{\mathbf{B}}} \int_F h_F \left|\mu(x,\boldsymbol{\xi})(\mathbf{grad}\ \Omega^{hi_0,P}(x,\boldsymbol{\xi}) - \mathbf{H}_s(x))\cdot\mathbf{n}(x)\right|^2 ds\end{aligned} \tag{85}$$

evaluates the discontinuity of the normal component of the magnetic flux density at the interior facets of tetrahedral elements, and the verification of the boundary conditions. This part represents so in some way the error coming from the spatial discretization and is called the spatial part of the estimator. The second part related to

$$\eta^2_{sto}(\boldsymbol{\xi}) = \mathbf{r}^t(\boldsymbol{\xi})\boldsymbol{\Lambda}_0^{-1}\mathbf{r}(\boldsymbol{\xi}) \tag{86}$$

represents the error coming from the stochastic discretization, so called the stochastic part of the estimator.

4.4. Efficiency of the error estimator

In this section, following the work [27], we aim to prove the local efficiency of the estimator (57).

Lemma 8 (**Bubble functions**). *For a given facet F of the mesh $\mathcal{T}_h$, we introduce $\gamma(F)$ the set of elements having F as a facet ($\gamma(F)$ contains 2 elements if F is an interior facet and one element if F is located on the boundary of the domain D). The facet bubble functions (see [27]) $\psi_F(x) : \gamma(F) \mapsto \mathbb{R}$ vanishes on all facets excepting on the facet F and is non zero in the interior of $\gamma(F)$. Let G^k_F be a polynomial functional space defined on the facet F whose order is lower than k.*

We have, for any $v \in G^k_F$:

$$C\int_F v^2(x)\,ds \le \int_F \psi_F(x)v^2(x)\,ds \le C\int_F v^2(x)\,ds, \tag{87}$$

Moreover, there exists an extension $\overline{v}$ *of* v *to* $\gamma(F)$ *such that:*

$$h_F^{-\frac{1}{2}}\sqrt{\int_{\gamma(F)}\psi^2(x)\overline{v}^2(x)\,dx}+h_F^{\frac{1}{2}}\sqrt{\int_{\gamma(F)}(\mathbf{grad}\ (\psi(x)\overline{v}(x)))^2\,dx}\leq C\int_F\overline{v}^2(x)\,dx. \tag{88}$$

Proof. See [16]. □

Lemma 9. *We have:*

$$\sqrt{\frac{1}{\mu^0_{max}}}\eta_{spa}(\boldsymbol{\xi})\leq C\,e_{glo}(\boldsymbol{\xi}). \tag{89}$$

Proof. For any $v\in V_x\otimes V_{\boldsymbol{\xi}}$ by using (33), we can deduce that:

$$\begin{aligned}&\int_D\mu(x,\boldsymbol{\xi})\mathbf{grad}\ \boldsymbol{\varepsilon}'_{glo}(x,\boldsymbol{\xi})\cdot\mathbf{grad}\ v(x,\boldsymbol{\xi})\,dx\\ &=\int_D\mu(x,\boldsymbol{\xi})\mathbf{grad}\ \Omega^{h0,P}(x,\boldsymbol{\xi})\cdot\mathbf{grad}\ v(x,\boldsymbol{\xi})\,dx\\ &-\int_D\mu(x,\boldsymbol{\xi})\mathbf{H}_s(x)\cdot\mathbf{grad}\ v(x,\boldsymbol{\xi})\,dx.\end{aligned} \tag{90}$$

By applying an integration by part, and due to (74), we obtain:

$$\begin{aligned}&\int_D\mu(x,\boldsymbol{\xi})\mathbf{grad}\ \boldsymbol{\varepsilon}'_{glo}(x,\boldsymbol{\xi})\cdot\mathbf{grad}\ v(x,\boldsymbol{\xi})\,dx\\ =\ &\int_{F\in\Delta_{in}}R_F(x,\boldsymbol{\xi})v(x,\boldsymbol{\xi})\,ds+\int_{F\in\Delta_{\mathbf{B}}}R_n(x,\boldsymbol{\xi})v(x,\boldsymbol{\xi})\,ds,\end{aligned} \tag{91}$$

where

$$R_F(x,\boldsymbol{\xi})=\left[\mu(x,\boldsymbol{\xi})(\mathbf{grad}\ \Omega^{h0,P}(x,\boldsymbol{\xi})-\mathbf{H}_s(x))\right]_F$$

and

$$R_n(x,\boldsymbol{\xi})=\mu(x,\boldsymbol{\xi})(\mathbf{grad}\ \Omega^{h0,P}(x,\boldsymbol{\xi})-\mathbf{H}_s(x))\cdot\mathbf{n}(x). \tag{92}$$

We are first interested in an interior facet F. We can notice that $\psi_F R_F$ can be extended to $\psi_F\overline{R_F}$ defined on the whole domain D where $\psi_F(x)\overline{R_F}(x,\boldsymbol{\xi})=0$ if x is located outside of $\gamma(F)$ such that $\psi_F\overline{R_F}$ is piecewise polynomial and

globally continuous on D. Then $\psi_F\overline{R_F} \in V_x \otimes V_{\boldsymbol{\xi}}$. By replacing v in (91) by $\psi_F\overline{R_F}$ we obtain:

$$\int_{\gamma(F)} \mu(x,\boldsymbol{\xi})\mathbf{grad}\ \boldsymbol{\varepsilon}'_{glo}(x,\boldsymbol{\xi}) \cdot \mathbf{grad}\ (\psi_F(x)\overline{R_F}(x,\boldsymbol{\xi}))\, dx \tag{93}$$

$$= \int_F \overline{R_F}(x,\boldsymbol{\xi})\psi_F(x)\overline{R_F}(x,\boldsymbol{\xi})\, dx. \tag{94}$$

By applying the Cauchy-Schwarz inequality, we obtain:

$$\int_{\gamma(F)} \mu(x,\boldsymbol{\xi})\mathbf{grad}\ \boldsymbol{\varepsilon}'_{glo}(x,\boldsymbol{\xi}) \cdot \mathbf{grad}\ (\psi_F(x)\overline{R_F}(x,\boldsymbol{\xi}))\, dx$$

$$\leq \left(\int_{\gamma(F)} \mu(x,\boldsymbol{\xi})|\mathbf{grad}\ \boldsymbol{\varepsilon}'_{glo}(x,\boldsymbol{\xi})|^2\, dx\right)^{\frac{1}{2}} \tag{95}$$

$$\times \left(\int_{\gamma(F)} \mu(x,\boldsymbol{\xi})|\mathbf{grad}\ (\psi_F(x)\overline{R_F}(x,\boldsymbol{\xi}))|^2\, dx\right)^{\frac{1}{2}}.$$

We can also notice that for each value of $\boldsymbol{\xi}$, $\overline{R_F}(\cdot,\boldsymbol{\xi}) \in G^1_F$. Therefore, by applying (87) and (88) we obtain:

$$\int_{\gamma(F)} \mu(x,\boldsymbol{\xi})|\mathbf{grad}\ (\psi_F(x)\overline{R_F}(x,\boldsymbol{\xi}))|^2\, dx$$

$$\leq \mu_F^{max}(\boldsymbol{\xi}) \int_{\gamma(F)} |\mathbf{grad}\ (\psi_F(x)\overline{R_F}(x,\boldsymbol{\xi}))|^2\, dx \leq Ch_F^{-1}\mu_F^{max}(\boldsymbol{\xi}) \int_F \overline{R_F}^2(x,\boldsymbol{\xi})\, ds \tag{96}$$

and:

$$\int_F R_F^2(x,\boldsymbol{\xi})\, ds \leq C \int_F R_F(x,\boldsymbol{\xi})\psi_F(x)R_F(x,\boldsymbol{\xi})\, ds, \tag{97}$$

where $\mu_F^{max}(\boldsymbol{\xi})$ is the maximum value among the two permeabilities of the two adjacent elements of $\gamma(F)$. From (94), (95), (96) and (97) we can deduce that:

$$\frac{1}{\mu_F^{max}(\boldsymbol{\xi})} \int_F h_F R_F^2(x,\boldsymbol{\xi})\, ds \leq C \int_{\gamma(F)} \mu(x,\boldsymbol{\xi})|\mathbf{grad}\ \boldsymbol{\varepsilon}'_{glo}(x,\boldsymbol{\xi})|^2\, dx. \tag{98}$$

Considering a facet F' located on the boundary of D, by using the same arguments, we can obtain:

$$\frac{1}{\mu_T(\boldsymbol{\xi})} \int_{F'} h_{F'} R_n^2(x, \boldsymbol{\xi})\, ds \leq C \int_{T(F')} \mu(x, \boldsymbol{\xi}) |\mathbf{grad}\ \boldsymbol{\varepsilon}'_{glo}(x, \boldsymbol{\xi})|^2\, dx, \tag{99}$$

where $T(F')$ is the element having F' as facet and $\mu_T(\boldsymbol{\xi})$ is the permeability in the element T. From (98), (99) and (85) and due to the fact that the permeability is bounded (see (18)) and $\mathbf{grad}\ \Omega^{hi_0,P}(x, \boldsymbol{\xi}) = \mathbf{grad}\ \Omega^{h0,P}(x, \boldsymbol{\xi})$, Lemma 9 is proved. □

Lemma 10. *We have:*

$$\sqrt{k_1}\eta_{sto}(\boldsymbol{\xi}) \leq e_{glo}(\boldsymbol{\xi}). \tag{100}$$

Proof. We can easily deduce from (19) and (34) that:

$$e^2_{glo}(\boldsymbol{\xi}) = e^2_{sto}(\boldsymbol{\xi}) + \int_D \mu(x, \boldsymbol{\xi}) |\mathbf{grad}\ (\Omega^{h0}(x, \boldsymbol{\xi}) - \Omega(x, \boldsymbol{\xi}))|^2\, dx. \tag{101}$$

We conclude the proof by using Theorem 1. □

Theorem 3.

$$\sqrt{k_1}\eta_{sto}(\boldsymbol{\xi}) + \sqrt{\frac{1}{\mu^0_{max}}}\eta_{spa}(\boldsymbol{\xi}) \leq C\, e_{glo}(\boldsymbol{\xi}). \tag{102}$$

Proof. Direct consequence of Lemmas 9 and 10. □

5. Numerical example

We now perform some numerical simulations to underline the estimator behavior. We are interested in the following magnetostatic example. The domain D is splitted into 5 sub-domains with the relative permeabilities $\mu_0 = 1$, $\mu_1 = \mu_2 = 1000$, and μ_3 and μ_4 are two independent uniform random variables defined in the range [600 - 1400]. This test is a benchmark allowing to illustrate our theoretical results. Nevertheless, in real cases, the number of random variables should be significantly larger. The current $|\mathbf{J}_s|$ is imposed equal to 1A. We use the SSFEM method associated to Legendre polynomial chaos expansion with the scalar potential formulation [19, 12] to solve this stochastic problem. In the SSFEM method, the obtained solution depends

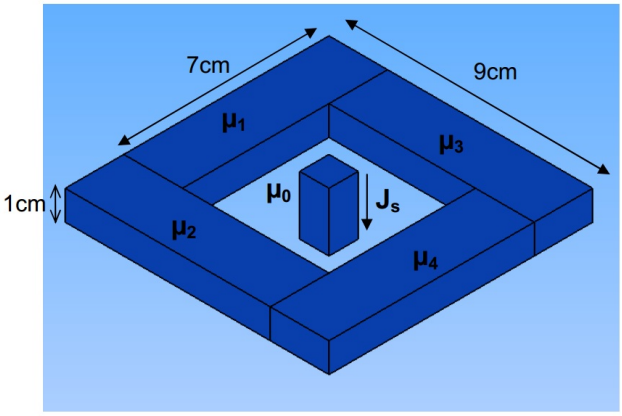

Figure 2: Stochastic magnetostatic problem.

on the spatial mesh size parameter h as well as on the order of the polynomial chaos and the accuracy of the solution of the linear system (23). Therefore, the numerical error also depends on these three factors. Here, the system (23) is solved by a conjugate gradient method and the accuracy of the numerical solution of (23) is evaluated by a stopping criterion R based on the residual of (23). We are interested at first in the mean value of the stochastic error with a fixed mesh of 2617 nodes (Fig. 3). With a given numerical solution $\Omega^{hi_0,P}$

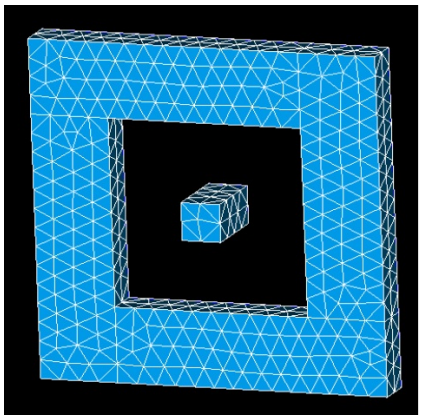

Figure 3: Mesh with 2617 nodes.

the mean value of the stochastic estimator (40) is compared to the mean value of the stochastic error approximated by the Monte-Carlo method with 1000 samples which process is described in Fig. 4. In Fig. 5 (similar to

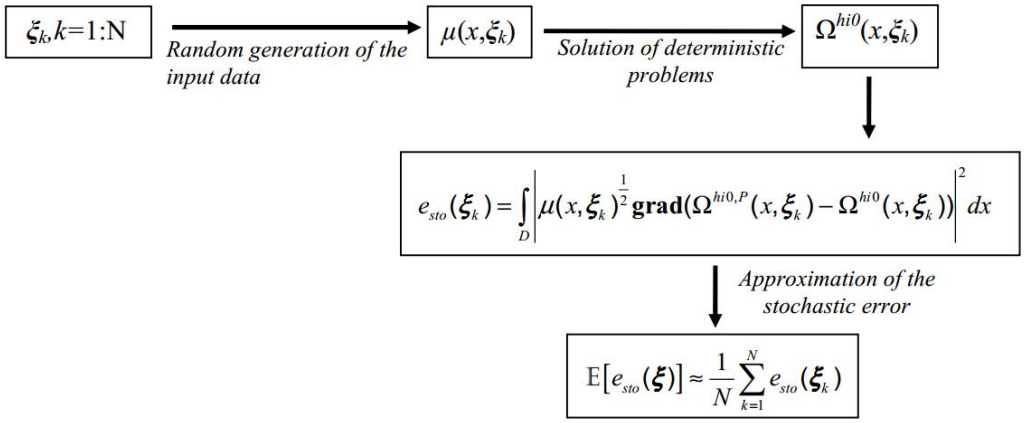

Figure 4: Mean value of the stochastic error obtained by the Monte-Carlo method.

Fig. 3 in [22]), we plot the evolution of the mean stochastic estimator (40) and the stochastic error estimated by the Monte-Carlo method (see Fig. 4) as a function of the order of polynomial chaos and of the accuracy of the solution of the linear system (23). From Fig. 5, some informations can be deduced : 1. The estimator and the approximated stochastic error obtained by the Monte-Carlo method are very close. 2. While the accuracy level of the solution of the linear system (23) is low (R is upper than 10^{-4} in Fig. 5) the stochastic error is the same with different orders of truncated polynomial chaos decomposition. 3. While the accuracy level is high enough (R is lower than 10^{-4} in Fig. 5) a higher order of polynomial chaos yields a smaller stochastic error. 4. With a given order of polynomial chaos, when the accuracy level increases, the evolution of the stochastic error decreases up to a given value before being stable ($log(R) = -6$ with order $P = 2$ and $log(R) = -8$ with order $P = 4$). Then, it is wasteful to increase the accuracy level of the solution of the linear system (23) beyond these points.

We are interested now in the spatial estimator (85). The order of the polynomial chaos is fixed equal to 4. At first, we use the mesh presented in Fig. 3. Then, the obtained numerical solution $\Omega^{hi_0,P}$ depends only on the stopping criterion R of (23). For each value of R, the mean value of the spatial estimator (85) and of the stochastic estimator (86) are evaluated. In Fig. 6, we plot the evolution of the mean value of spatial estimator in function of the mean value of the stochastic estimator. One can notice that when the stochastic estimator is small enough (10^{-2} in this example), with

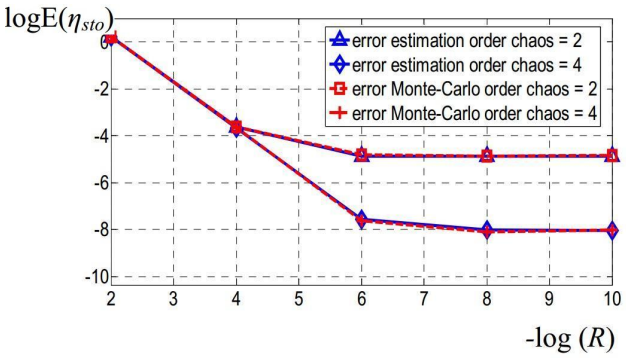

Figure 5: Stochastic estimator and estimated stochastic error in function of order of polynomial chaos and of the stopping criterion R.

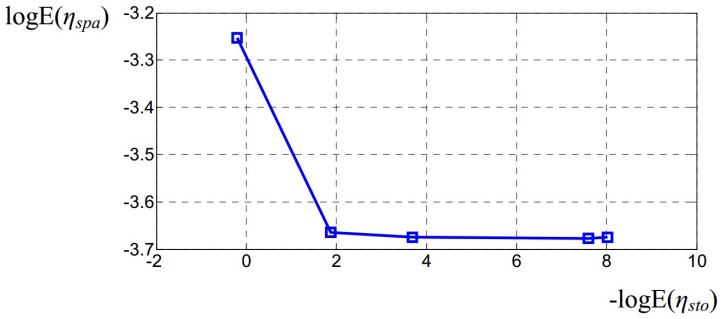

Figure 6: Spatial error estimation in function of stochastic error estimation .

a given mesh, the mean value of (85) seems to be stable. The stability of the mean value of the spatial estimator can be explained by the fact that when

the stochastic error is small enough, we can consider that:

$$\begin{aligned}
&\sum_{F\in\Delta_{in}}\int_F h_F\left[\mu(x,\boldsymbol{\xi})(\mathbf{grad}\ \Omega^{hi_0,P}(x,\boldsymbol{\xi})-\mathbf{H}_s(x))\right]_F^2\ ds\\
&+\sum_{F\in\Delta_{\mathbf{B}}}\int_F h_F\left(\mu(x,\boldsymbol{\xi})(\mathbf{grad}\ \Omega^{hi_0,P}(x,\boldsymbol{\xi})-\mathbf{H}_s(x))\mathbf{n}(x)\right)^2\ ds\\
\approx\ &\sum_{F\in\Delta_{in}}\int_F h_F\left[\mu(x,\boldsymbol{\xi})(\mathbf{grad}\ \Omega^{hi_0}(x,\boldsymbol{\xi})-\mathbf{H}_s(x))\right]_F^2\ ds\\
&+\sum_{F\in\Delta_{\mathbf{B}}}\int_F h_F\left(\mu(x,\boldsymbol{\xi})(\mathbf{grad}\ \Omega^{hi_0}(x,\boldsymbol{\xi})-\mathbf{H}_s(x))\mathbf{n}(x)\right)^2\ ds.
\end{aligned}\tag{103}$$

The right hand side of (103) only depends on the mesh and it can be shown [8] that the right hand-side of (103) is an equivalent measure of the spatial error evaluating the distance between $\mathbf{grad}\ \Omega^{hi_0}(x,\boldsymbol{\xi})$ and $\mathbf{grad}\ \Omega(x,\boldsymbol{\xi})$.

We are finally interested in the numerical solution $\Omega^{hi_0,P}$ obtained by using the different meshes. In Fig. 7 we can notice that with a given order of polynomial chaos ($P=4$) and a given R, the stochastic estimator (86) depends on the mesh because $\Omega^{hi_0,P}$ and Ω^{hi_0} are mesh dependent. However, when the stopping criterion R is small enough, it seems to be independent on the mesh (the lowest curve in Fig. 7). Figure 8 represents the evolution

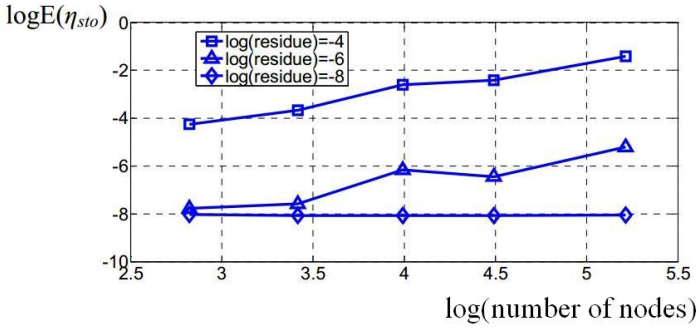

Figure 7: Stochastic error estimation in function of number of nodes, order of polynomial chaos $P=4$.

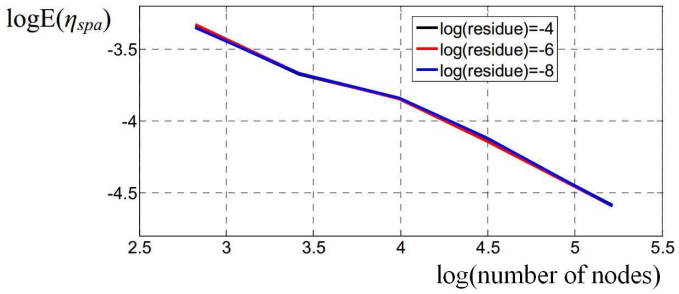

Figure 8: Spatial error estimation in function of of number of nodes.

of the mean value of the spatial error estimator (85) as a function of the number of nodes of the mesh and of the value of R. One can notice that the mean value of the spatial estimator depends only on the mesh and is almost independent on the approximation in the stochastic dimension since the error does not depend on the value of R.

6. Conclusion

In this paper we have presented an a *posteriori* error estimation for a stochastic magnetostatic problem. The error estimator is decomposed into two terms, one depending on the stochastic discretization and one depending on the spatial discretization and on the stochastic discretization. Nevertheless, we have observed on the example that the last term depends only on the spatial accuracy provided that the approximation in the stochastic dimension is sufficiently accurate.

The residual-based error estimator has been developed for an approximation in the stochastic dimension based on a truncated polynomial chaos expansion. The strategy can also be applied for other kinds of approximation spaces based on wavelets or piecewise polynomials for example. The proposed error estimator can be used to compare the accuracy of the different approximation spaces and numerical methods by evaluating the two parts of the estimator (spatial and stochastic one). It enables also to make a relative comparison in terms of accuracy between the spatial errors and the stochastic errors.

Acknowledgement This work is supported by the program MEDEE funded by the Nord Pas de Calais council and the European Community and is

supported in part by the Labex CEMPI (ANR-11-LABX-0007-01).

References

[1] M. Ainsworth, J. T. Oden. A posteriori error estimation in finite element analysis, Comput. Methods Appl. Mech. Engrg, vol. 142, pp. 1-88, 1997.

[2] I. Babuska, P. Chatzipantelidis. On solving elliptic stochastic partial differential equations. Computer Methods in Applied Mechanics and Engineering, 191:4093-4122, 2002.

[3] I. Babuska, W.C. Rheinboldt. A posteriori error estimates for the finite element method, Internat. J. Numer. Methods Engrg, vol. 12, pp. 1597-1615, 1978.

[4] I. Babuska, W.C. Rheinboldt. A posteriori error analysis of finite element solutions for one dimensional problems, SIAM J. Numer. Anal, vol. 18, pp. 565-589, 1981.

[5] I. Babuska, T. Strouboulis. The finite element method and its reliability, Oxford University Press, 2001.

[6] I. Babuska, R. Tempone, G. Zouraris. Galerkin finite element approximations of stochastic elliptic partial differential equations, SIAM Journal on Numerical Analysis, 42:800-825, 2004.

[7] I. Babuska, R. Tempone, G. Zouraris. Solving elliptic boundary value problems with uncertain coefficients by the finite element method : the stochastic formulation, Computer Methods in Applied Mechanics and Engineering, 194:12511294, 2005.

[8] R.E. Bank. Hierarchical bases and the finite element method, Acta Numer, vol. 5, pp. 143, 1996.

[9] R.E. Bank, A. Weiser. Some a posteriori error estimators for elliptic partial differential equations, Math. Comp, vol. 44, pp. 283301, 1985.

[10] R. Becker, H. Kapp, R. Rannacher. Adaptive finite element methods for optimization problems, Proceedings of 18th Biennial Conference on Numerical Analysis, pp. 21-42, Chapman and Hall/CRC, 2000.

[11] K. Beddek, S. Clenet, O. Moreau, V. Costan, Y. Le Menach, A. Benabou. Adaptive Method for Non-Intrusive Spectral Projection - Application on a Stochastic Eddy Current NDT Problem. IEEE Trans on Magn, vol. 48 , issue 2, pp. 759 - 762, 2012.

[12] K. Beddek, Y. Le Menach, S. Clenet, O. Moreau. 3D spectral finite element in static electromagnetism using vector potential formulation, IEEE Trans on Magn, vol. 47, pp. 1250-1253, 2011.

[13] G. Blattman, B. Sudret. Sparse polynomial chaos expansions and adaptive stochastic finite elements using a regression approach, C.R mcanique, vol. 336, issue 6, pp. 516-523, 2008.

[14] A. Bossavit. Computational electromagnetism, Academic Press (Boston), 1998.

[15] R.H. Cameron, W.T. Martin. The orthogonal development of non linear functionals in series of Fourier-Hermite functionals, Annal of mathematics, vol. 48, no. 2, pp. 385-392, 1947.

[16] P. Clement. Approximation by finite element funcitons using local regularization, RAIRO Anal. Numer., vol. 9, pp. 77-84, 1975.

[17] S. Clenet, N. Ida. Error Estimation in a Stochastic Finite Element Method in electrokinetics, Int. J. Numer. Mth. Engng, vol. 81, no. 11, pp. 1417-1438, 2010.

[18] M. Deb, I. Babuska, J. Oden. Solution of stochastic partial differential equations using galerkin finite element techniques, Computer Methods in Applied Mechanics and Engineering, 190: 6359-6372, 2001.

[19] R. Gaignaire, S. Clenet, O. Moreau, B. Sudret. 3D spectral stochastic finite element method in electromagnetism, IEEE Trans on Magn, vol. 43, no. 4, pp. 1209-1212, 2007.

[20] R. Ghanem, P. Spanos. Stochastic finite elements: a spectral approach, Springer-Verlag, Berlin, 1991.

[21] O. Le Maitre, O. Knio, H. Najm, R. Ghanem. Adaptive multi-wavelets decomposition for stochastic processes, ICOSAHOM, Brown University, Providence RI, June 21-25, 2004.

[22] H. Mac, S. Clenet. A posteriori error estimation for stochastic static problem, IEEE Trans on Magn, vol. 50, issue 2, pp. 545-548, 2014.

[23] L. Mathelin, O. Le Matre. Dual based a posteriori error estimate for stochastic finite element methods, COMM. APP. MATH. AND COMP. SCI, vol. 2, no. 1, pp. 83-115, 2007.

[24] W. Prager, J.L. Synge. Approximations in elasticity based on the concept of function space, Q. App. Math, vol. 5, pp. 241-269, 1947.

[25] L.R. Scott, S. Zhang. Finite element interpolation of non-smooth functions satisfying boundary conditions, Math. Comput, vol. 54, pp. 483-493, 1992.

[26] I. Tsukerman. Computational Methods for Nanoscale Apllications Particles, Plasmons and Waves, Nanostructure science and technology, Springer 2007.

[27] R. Verfurth. A posteriori error estimation and adaptive mesh refinement techniques, J. Comput. Appl. Math, vol. 50, pp. 67-83, 1994.

[28] X. Wanand, G. E. Karniadakis. Error Control in Multi-Element Generalized Polynomial Chaos Method for Elliptic Problems with Random Coefficients, Communications in Computational Physics, vol. 5, no. 2-4, pp. 793-820, 2009.

[29] D. Xiu., G. Karniadakis. The Wiener-Askey polynomial chaos for stochastic differential equations, SIAM J.Sci. Comput, vol. 24, pp. 619-644, 2002.

[30] O.C. Zienkiewicz, J.Z. Zhu. The superconvergent patch recovery and a posteriorierror estimates. Part 1: The recovery technique, Int. J. Numer. Methods Engrg, vol. 33, pp. 1331-1364, 1992.

[31] O.C. Zienkiewicz, J.Z. Zhu. The superconvergent patch recovery and a posteriorierror estimates. Part 2: Error estimates and adaptivity, Int. J. Numer. Methods Engrg, vol. 33, pp. 1331-1364, 1992.